Field-induced columnar structures in a quasi-two-dimensional system of dipolar particles

Shin-Shing Yeh, Ching Hsueh, and Peilong Chen
Department of Physics and Center for Complex Systems, National Central University, Chungli 320, Taiwan

Jorge Viñals
McGill Institute for Advanced Materials and Department of Physics, McGill University, Montreal, QC H3A 2T8, Canada

(Received 12 February 2007; revised manuscript received 3 September 2007; published 29 November 2007)

We study the formation of columnar structures of uniaxial dipoles in an external magnetic field both experimentally and theoretically. By applying an external magnetic field parallel to a thin layer of a magnetorheological fluid, we manipulate a single initial cluster of suspended colloidal particles. We find that the cluster breaks up into columns that have approximately uniform widths and intercolumnar spacings. Both the average column width and inter column spacing are observed to vary linearly with column length. The observed linear relationships between column width and spacing versus the column length are interpreted theoretically by computing the potential energy of an ensemble of closed-packed columns of spherical dipolar particles.

DOI: 10.1103/PhysRevE.76.051407 PACS number(s): 82.70.Dd, 75.50.Mm

I. INTRODUCTION

Colloids exhibit various structures and phase behavior depending on interparticle interactions [1]. When applying an external field to electrorheological (ER) or magnetorheological (MR) fluids/ferrofluids which couple, respectively, to electric or magnetic fields, dipole moments are induced due to the difference in dielectric constants or magnetic permeabilities between the particles and surrounding buffers. Typically ferrofluids contain nanometer-scale "superparamagnetic" particles, while in MR fluids the particles are micrometerscale, thus leading to much more significant thermally driven motion in ferrofluids. If the dipolar interaction between particles is strong enough, the suspensions can undergo structural transitions, for example, from randomly dispersed particles to clusters. The resulting dramatic changes in rheological response due to the structural transition lead to many technological applications, and have attracted much attention recently [2].

Study of these structures under external fields is fundamental in understanding the properties and response to shears of ER and MR fluids. Under an electric field, suspensions of ER fluids were observed to form chains quickly, then aggregate into thick columns [3,4]. In addition to standard dipole-dipole interactions between two infinitely long dipolar chains, attractive forces originating from thermal chain fluctuations have also been obtained [5]. For a thick column the ground state was demonstrated to be a body-centered tetragonal (bct) lattice, both theoretically and experimentally [4,6]. Analogous structures have also been found in MR fluids [7–9]. In practice, however, the use of MR fluids or ferrofluids avoids some complicating factors that hamper the investigation of the structural evolution in ER fluids, such as surface charge, electrode polarization, and adsorbed water. The different behavior of ER and MR fluids is mainly due to their different boundary conditions. For example, in the absence of image dipoles in MR fluids, the interaction among chains and columns strongly depends on the their finite length.

Most experiments to date that study field induced structures in MR fluids or ferrofulids apply a slowly increasing field that is perpendicular to a thin sample film, so that thermal motion allows particles and chains to find their more stable configurations. Under a strong magnetic field, columnar structures parallel to the field were found, and two-dimensional periodic patterns were observed [7–10]. Both spacing and width of these columns were observed to depend sensitively on the dimensions of the experimental cell, and to obey scaling relations. However, the scaling exponents between the diameter and the length of the cylindrical columns (the latter is set by the spacing between the two glass plates between which the samples are filled) were seen to depend on certain details of the system in mostly ferrofluid samples, with conflicting values of 0.67 [7], 0.37 [8], and even a transition between two regimes has been reported [9,10]. Several theories have been advanced to explain the experimental results by minimizing the appropriate free energy, but different assumptions of ellipsoidal [3,7] and cylindrical [8,10] column shapes lead to different values of the exponents.

A few experiments have involved the application of a magnetic field parallel to a thin sample to study structure evolution in MR fluids [11,12] and ferrofluids [13]. Macroscopic one dimensional patterns were only found in an oscillating magnetic field within a small range of frequencies [11]. In a dc field, only needlelike structures were found in nonequilibrium states [12,13]. Although two-dimensional Monte Carlo simulations were used to describe the observed thick chainlike clusters [14], their width was not related to the length of the chains. So far columnar sizes and intercolumnar spacings in two-dimensional thin films have not been studied systematically, neither theoretically nor experimentally.

In this paper, we study the formation of columnar structures in a thin film of a MR fluid both experimentally and theoretically. Unlike prior experiments, the MR fluid is inside a thin, approximately flat glass tube. An external magnetic field is applied along the direction parallel to the film, such that the length of resulting columns is set by the inner tube dimension. We then study the breakup of large colloidal particle aggregates under the application of the external field, rather than applying the field to a colloidal suspension of

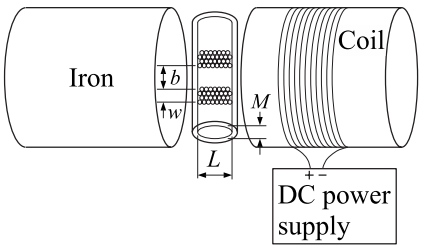

FIG. 1. The experimental setup shows the glass tube with an elliptical cross section in the center. The diameter of the iron cores is 6.5 cm, and the gap between them is 2 cm. For clarity, the cross section of the glass sample cell and sizes of the dipolar particles are not drawn in scale.

uniform density, and obtain a linear array of columns with a definite column length. By varying the geometry of the initial aggregate and the experimental cell, we show that the resulting column widths and intercolumn spacings are independent of the film thickness. The observed average column width and inter column spacing in final steady states are proportional to the column length (set by the tube dimensions). We then model the columns as comprised of spherical dipolar particles arranged in a two-dimensional (2D) closed packed lattice, or in a three-dimensional (3D) lattices of small cross section with two different packing configurations. The column widths minimizing the total dipole-dipole potential energy are computed and they are found to be proportional to its length, as in the experiments. By computing the potential energy between two columns, we also provide an interpretation of the dynamically selected column separations.

II. EXPERIMENTAL SETUP AND PROCEDURE

Figure 1 shows our experimental setup that consists of a glass sample cell, an electromagnet made by a coil wound around an iron cylinder and connected to a dc power supply, and a CCD camera. The column geometry is indicated as the column length L, column width w, and column spacing b. The third dimension of the column will be called the column thickness, although not illustrated in the figure. The magnetized cylinder produces a magnetic field with an average value of 570 G/A at the midsection along its axis. The samples are contained in glass tubes with approximately elliptical inner cross sections. A variety of tubes have been used with cross section dimensions ($L \times M$) at (340×209), (637×303), (660×210), (666×318), (705×328), (734×354), (918×409), (951×440), (1539×395), and (1800×361) in (μm $\times$ μm).The ratio of M/L is in the range between 0.2 to 0.5. The external magnetic field is directed along the long axis of the ellipsoid, parallel to the L direction.

The suspensions used in our experiments, Dynalbeads M-450 Epoxy manufactured by the Dynal A.S company, are made of Fe_3O_4 particles coated by Styrofoam. Each Fe_3O_4 grain corresponds to a single magnetic domain. In the absence of an external magnetic field, the magnetic dipoles in each particle are randomly oriented in the suspension due to thermal motion. The particle is thus superparamagnetic and does not exhibit hysteresis. The whole droplet with the Fe_3O_4 core has a mean diameter of about $d=4.5$ μm, with polydispersivity less than 4%, and a susceptibility $\chi=0.24$. To prevent aggregation due to van der Waal's attraction before applying a magnetic field, the droplets are dissolved in dilute 0.001 M NaOH solution to provide an interparticle repulsion. Typically the induced interaction between Dynalbeads at $pH=11$ is large enough to avoid aggregation [16].

The strength of the dipolar interaction can be characterized by a coupling constant λ

$$\lambda = \frac{U_{d-d}}{k_B T} = \frac{\pi \mu_0 d^3 \chi^2 H^2}{72 k_B T}, \tag{1}$$

where U_{d-d} is the interaction energy between two particles in contact with dipoles aligned along the field direction, k_B the Boltzmann constant, T the temperature, μ_0 the magnetic permeability of free space, d the particle diameter, χ magnetic susceptibility of the particle, and H the external magnetic field. The external field in our experiments is at the order of 1000 G, i.e., $\lambda \approx 10^6 \gg 1$, thus the dipoles are expected to form stable chains and columns. The magnetic force is also significantly larger than the steric repulsion and Van der Waal's attraction, therefore dominating the formation of chains.

Experimentally determining the equilibrium state of a dipolar fluid with micro millimeter-sized particles is often difficult because the system can easily be trapped in metastable states. For example, chains or small columns tend not to aggregate into larger ones due to the potential barriers caused by the long ranged repulsion of the dipole-dipole interaction. Hence the column size is often smaller than that of the equilibrium state. To mitigate this difficulty in our experiments, we have chosen to observe the breakup of an initial large aggregate under the field instead of directly studying the formation of columns from a uniform suspension. Figure 2(a) shows the initial state prepared as a single aggregate by manipulating the particles with magnetized tweezers at zero field.

The sample is then placed in a magnetic field of slowly increasing magnitude to observe the break up of the aggregate into columns. Figure 2(b) shows the static periodic pattern that results after several minutes when the field reaches 2000 G. We next reassemble the columns by placing a weakly magnetized clip near the sample, as shown in Fig. 2(c). Some of the larger columns then break into smaller ones. After removing the clip, we repeat the process of increasing the field slowly to reach the final steady state shown in Fig. 2(d). As can be seen in the figures, the initial breakup of the aggregate in (b) typically has smaller column spacings and also larger variations. Repeated application of the magnetized clip leads to stable and more uniform column spacing as seen in (d). For the statistical analysis of column configurations, we collect distributions of column width w, and intercolumn spacing b from the recorded images. In this final state, the outermost columns (marked as A in the figure) are often much narrower than those in the center. This is probably due to the uneven edges of the initial aggregate in Fig. 2(a), and to edge effects in the dipole dipole interaction. We

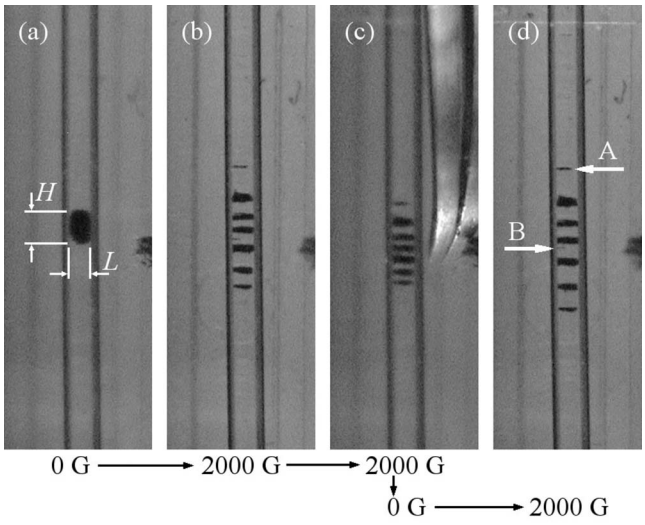

FIG. 2. (a) The aggregate used as the initial state. (b) A steady state as the slowly increasing field reaches 2000 G. (c) Columns being assembled by a magnetized clip. (d) The final steady state after removing the clip, turning off the field, and slowly increasing the field again. The width of the glass tube is 666 μm.

also observe sometimes inhomogeneities within the column ensemble [marked as *B* in Fig. 2(d)], in the form of thinner columns lying between two wide columns. Both types of outliers in the distribution of widths are ignored. Finally, we mention that the spacing b between the columns is often slightly larger near the two ends of the sample compared to the central region. This should also be and end effect where the columns at the sample ends experience repulsion from only one side.

We have considered a number of tubes of different cross sections, and for each the measurement of column widths and spacings is repeated six times. Figure 3 shows an example of the corresponding distribution of w and b in a cell with $L=666$ μm and $M=318$ μm (the length of the columns is also L). The distributions are broad, although an average is clearly discernible, with fluctuations most likely due to the details of the column break up processes. Even though particles within a broad column experience the largest repulsive forces near its center, the column may split off center due to inevitable packing defects. Once separated, the resulting smaller columns are unlikely to recombine, hence leading to significant width fluctuations.

It should be noted that the columnar widths and inter column separations that are dynamically selected, and that appear to be stationary, do not correspond to a configuration in thermodynamic equilibrium. The reason is that in our experiments thermal energies for Brownian motion of 4.5-μm sized particles are too small compared with potential barriers of magnetic origin such as the dipolar repulsion between two parallel chains. Therefore by preparing the initial cluster as a large isolated aggregate, we are probably not probing configurations in thermodynamical equilibrium, but rather the transient dynamics of break up of the initial aggregate. On the other hand, as we will discuss later, we find that the geometries of the columns in the stationary state, such as their widths and separations, are determined solely by the column length. This is the case under the conditions that we have used (tubes with different geometries and cross section ratios), and different preparation of the aggregate (different initial thickness in the same tube). Although dipole-dipole interaction calculations will show that forces between two columns are always repulsive, it is very convincing that the system as shown in Fig. 2(d) has reached a steady state with definite columnar spacings and widths. The columns would remain fixed for at least a few hours, while the processes from Fig. 2(a)–2(d) take only a few minutes.

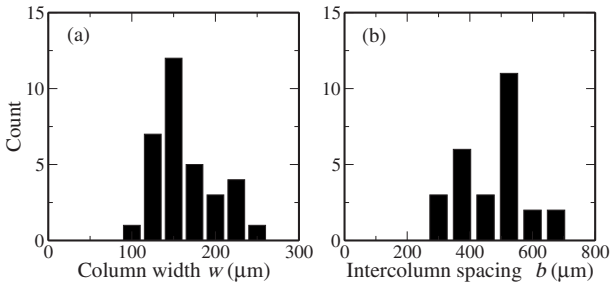

FIG. 3. Histograms of (a) column width w and (b) intercolumn spacing b, in a cell of a cross section dimension 666×318 μm^2.

III. THEORETICAL MODEL

In this section we discuss a simple model used to interpret the experimental observations that will be described in Sec. IV. We consider an ensemble of identical dipoles placed on a two-dimensional (2D) lattice of dimensions $L\times W$. In two dimensions, the lattice that will be used in the numerical solution of the model is comprised of two staggered square lattices forming a hexagonal lattice, as shown in Fig. 1. In the case of three-dimensional lattices, two different cases are considered: (i) a direct, aligned stacking of 2D hexagonal lattices and (ii) a close-packed bct lattice [4,6].

Dipoles attract when they are aligned with the field, thus leading to the formation of chains of length L. Staggered lattices allow a reduction in dipole dipole repulsion in the direction perpendicular to the applied field by having two successive chains out of register by one particle radius. Without this shift, the interaction between two chains is always repulsive, even for infinite long chains. With the shift, on the other hand, the interaction becomes attractive within a certain range of separations. Given that the range of this attractive interaction is shorter than twice the particle diameter d, even for long chains, a finite preferred width w of a multichain column is expected due to the competition between long-range repulsion and short-range attraction between the chains. Two-dimensional columnar structures are modeled as the close packed particle configurations on the lattice.

The potential energy of a configuration can be decomposed into three interaction parts: between pairs of dipoles within each chain of length L, between pairs of chains within each column, and within pairs of columns. The term arising from the pair interaction between dipoles inside a single chain remains constant once the total number of chains in the system is fixed. Since the total number of particles and the tube dimensions are fixed in our experiment, this contribution to the energy is a constant. Hence only the other two

interactions terms contribute to the determination of the columnar width and separation.

Consider the limiting case of a single column (e.g., low volume fraction of colloidal particles) comprised of w adjacent chains with chain lengths of L particles. Its magnetic energy is given by

$$\frac{U}{w} = \frac{1}{w}\sum_{k=1}^{w-1}(w-k)\beta_k, \tag{2}$$

where β_k is the pair interaction energy between chain one and its k_{th} neighboring chain. The variation f of Eq. (2) is

$$f = \triangle\left(\frac{U}{w}\right)/\triangle w = \frac{1}{w(w-1)}\sum_{k=1}^{w-1} k\beta_k. \tag{3}$$

It has been shown in Ref. [15] that β_k can be approximated as the sum of the interaction potential between two chains with infinite lengths ($L\to\infty$), and a finite size correction as

$$\begin{aligned} k\beta_k &= k\left(\frac{8\pi^2 L}{\sqrt{\rho_k}}e^{-2\pi\rho_k}\cos 2\pi s + \frac{2}{\sqrt{\rho_k^2+s^2}}\right. \\ &\quad \left. - \frac{1}{\sqrt{\rho_k^2+(L+s)^2}} - \frac{1}{\sqrt{\rho_k^2+(L-s)^2}}\right) \\ &\approx \frac{\sqrt{k}8\pi^2 L}{\sqrt{\rho_1}}e^{-2\pi\rho_k}\cos 2\pi s \\ &\quad + \frac{2}{\rho_1}\left[1+\left(\frac{s}{k\rho_1}\right)^2\right]^{-1/2} - \frac{2k}{L}\left[1+\left(\frac{k\rho_1}{L}\right)^2\right]^{-1/2}, \end{aligned} \tag{4}$$

where $\rho_k = k\sqrt{3}/2$, and s the relative vertical shift. Here all the lengths are scaled with the particle diameter d and energies with the energy between two particles in contact with aligned, unit dipole moments. In the second equation we have assumed $L \gg s$. The first term in the right hand side is much larger at $k=1$ than at $k>1$ due to the exponential decay with distance. The second term is approximately $2/\rho_1$ because $s/(k\rho_1) \ll 1$ when $k>1$. The third term is $-2k/L$ when $L \gg w$. Under these approximations, Eq. (3) becomes

$$f \approx -0.37L + 2.31w - w^2/L. \tag{5}$$

The preferred column width w_0 is obtained by requiring that $f=0$, and hence we find $w_0 \approx 0.17L$.

These results can be easily validated numerically, as shown in Fig. 4. The inset in the figure shows that the potential energy in the case of two dimensions has a minimum for a particular column width (similar results are obtained in three dimensions). The column width for which the potential energy is minimized is plotted versus column length in Fig. 4. The numerical results agree quite well with the asymptotic analytical calculation given above (the solid line in the figure) when $L/d > 100$. Numerical results for multiple columns will be presented in the next section.

IV. RESULTS AND DISCUSSION

We have first examined any effect deriving from the size of the initial aggregate prior to turning on the external field

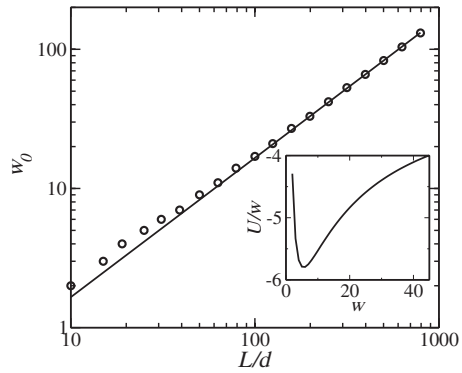

FIG. 4. Preferred number of chains w_0 in a column vs chain length L. The circles are computed numerically, and the solid line shows the asymptotic result with a slope of 0.17.

(see Fig. 1). At a fixed number of colloidal particles we can manipulate the initial aggregate [with dimensions denoted as $H \times L$ in Fig. 2(a)] to have different values of H, such that the aggregate does not fill up all the cell thickness M. Figure 5 shows our results for the steady state columnar width w (circles) and inter columnar spacing b in nonzero field as a function of H/L of the initial aggregate. Within errors, the steady state distribution of columns is seen to be independent of the initial condition.

When the initial aggregate fills up the cell thickness M, we can also analyze the effect on the steady state distribution of column widths and spacings by using two tubes with cross sections of similar L but different M. A weak dependence on M is observed. For example, the average columnar width in cells with cross sections $L=660$ μm and $M=210$ μm is $w=160\pm13$ μm, whereas we find in a cell of $L=666$ μm and $M=318$ μm that $w=173\pm5$ μm.

We next probe the interaction between two columns following the procedure illustrated in Fig. 6 to demonstrate that, as expected, it is always repulsive. Two neighboring columns from a steady state distribution are selected and isolated from the other columns [Fig. 6(a)]. They are then brought together by a magnetized clip as shown in Fig. 6(b). After removing the clip, the two columns regain their original separation, as shown in Fig. 6(c). On the other hand, if the spacing between

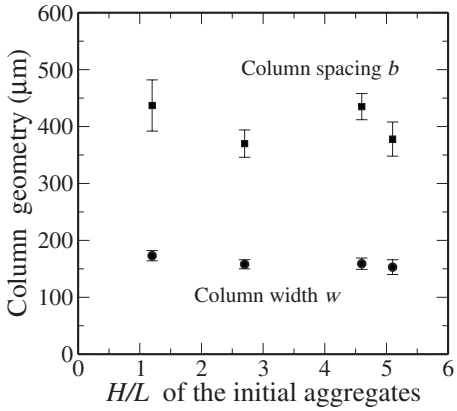

FIG. 5. Steady state average column width w (circles) and inter column spacing b (squares) for different geometries of initial aggregates.

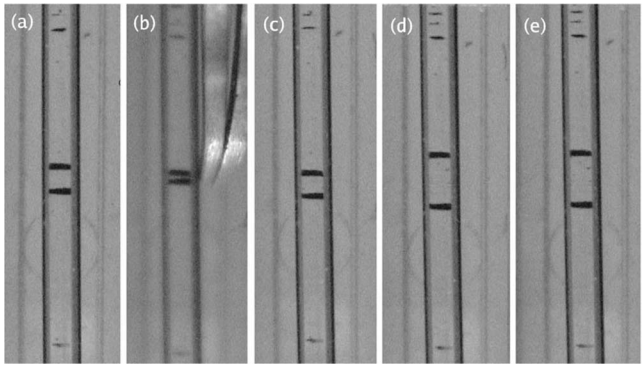

FIG. 6. Sequence of two column configurations used to probe their interaction. The width of the glass tube is 705 μm.

them is increased, as shown in Fig. 6(d), they remain at the larger separation [Fig. 6(e)]. This demonstrates that the intercolumn interaction is purely repulsive. However, two columns initially close by stop moving away from each other at some definite separation. We have not investigated the origin of the presumed friction force that leads to a stationary and finite inter column separation.

The repulsive interaction between pairs of columns accounts for the formation of an array of columns following the break up of an initial aggregate under an external field. The resulting average intercolumn spacing b is shown in Fig. 7 (column center to center distance) as a function of the chain length L. The distribution of column inter spacings appears to be stationary in the time scale of the experiment. In the figure, the circles correspond to data obtained by gradually increasing the magnetic field by using an electromagnet, whereas the squares correspond to the case in which an fixed external field is applied rapidly by placing the sample between two permanent magnets. The data show that the inter column spacing b for a gradually increasing field is very close to the column length L. On the other hand, the spacings obtained at constant applied field are slightly smaller, perhaps due to an insufficient relaxation time.

In order to interpret the existence of a finite intercolumn separation in steady state despite the fact that the dipole-

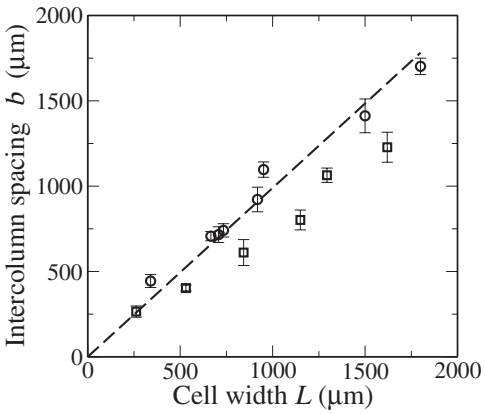

FIG. 7. Average intercolumn spacing b versus chain length L. The squares represent column formation at constant external field, and the circles at a slowly increasing field. The dashed line is a fit to the circles, yielding a slope of 1.

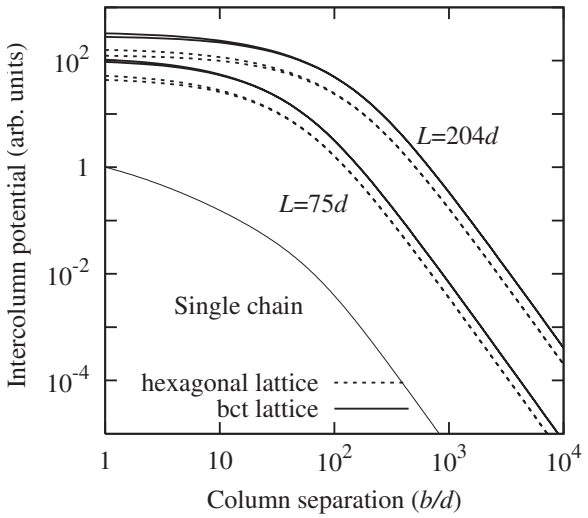

FIG. 8. Dipole-dipole energy, divided by the square of the column thickness, versus spacing between two identical columns. Except for the single chain, all data are obtained at column widths $w=L/3$. See text for explanation of further details.

dipole interaction between columns is always repulsive, and that $b \approx L$, we have calculated the potential energies of several configurations of two identical columns. Figure 8 shows our results for the potential energy as a function of inter column spacing b for column lengths $L=75d$ and $204d$. Given the actual particle diameter, these results correspond to cell dimension $L=340$ and 918 μm, respectively. Energies have been scaled with the square of the column thickness. Column widths have been fixed, and chosen to be either a single line of dipoles or $w=L/3$, the relation between column width and chain length seen in the experiments involving many columns (from Fig. 9). For each column length L, the dashed lines in Fig. 8 correspond to hexagonal packing, and the solid line to a bct lattice. For each packing, there are two lines (separated slightly at small separations, but the difference is not visible in the figure at the larger separations) indicate results for a single layer (the lower one) and for a layer with a finite thickness $=L/3$ (the upper one). The figure

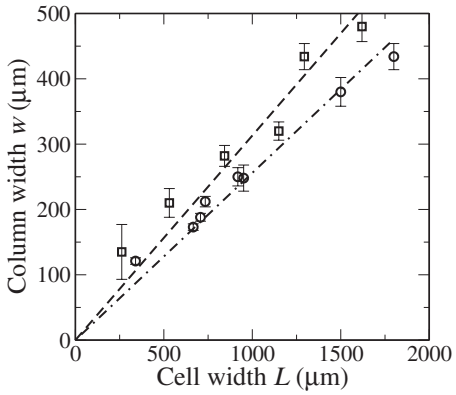

FIG. 9. Average column width w versus chain length L. The squares represent the case of a suddenly applied field. The circles represent the case of a slowly increasing field. The dashed and dot-dashed lines are linear fits to the data with slopes 0.31 and 0.26.

shows a very week dependence of the energy/(thickness)^2 on the thickness of the columns. Although the two different particle packings show different values of the energy at fixed L and W, the qualitative behavior in both cases is the same. For reference, we also show the interaction between two single chains with $L=75d$ in the figure.

The potential energy is seen to decay as $1/b^3$ at large spacings, as expected from the dependence of the interaction energy between two isolated dipoles. At shorter spacings, however, the interaction energy decays much more slowly. For the case of two single chain columns, the energy is seen to decay as $1/r$, a dependence that follows from β_k in Eq. (4). For wider columns, the decay is even slower. The results of Fig. 8 show that the experimentally determined values of $b \approx L$ lie in the crossover region of the potential energy between the slow decay at short distances, and the faster $1/r^3$ decay at long distances. This figure strongly suggests that two columns initially closer than the selected value of b move away from each other until reaching the crossover region of the potential energy. For larger distances, the repulsive force drops quickly and the columns are stabilized by mutual interactions with other columns, and ultimately by friction forces. At the very least, any residual column motion is too slow to be observable in the experiments. (It is noted that although the apparent magnitude of the slope is larger at larger separations, the slope does not directly equal to the force as the figure is plotted in the log-log scale.)

Figure 9 shows our results for the average column width w as a function of chain length L. Squares correspond to the case of a sudden application of a static magnetic field, whereas the circles represent the width attained after a gradual increase of the field over several minutes. In both cases, the column width w is seen to be proportional to the chain length L. A small change in the slope is observed depending on the preparation protocol: 0.26 for the case of a slowly increasing applied field and 0.31 for the case of column formation at constant magnetic field. We interpret the difference as being due to insufficient relaxation time for column break up at constant field relative to the other case.

To interpret these results, we have attempted the calculation of the total dipole-dipole energy $E(w,b)$ after an aggregate of N chains (with a uniform chain length L) breaks up into columns of equal width w, with a chosen and uniform column spacing b. Typically we use $N=20160$. Since the total energy depends on the column spacing b, i.e., how far the columns separate, the meaningful way of comparing energies with different column widths w is to make b depend on w such that $r=[(N/w)-1]b$ is fixed (N/w is the number of columns). Breaking into narrower columns (smaller w and hence more columns) leads to smaller b, and conversely for wider columns. The energy $E[w,b(w)]$ at fixed r exhibits a minimum at a particular width $w=w_m$. It is found that the minimum energy width w_m is not sensitive to the selected value of r. For the data shown below, the value of r used is such that the resulting column spacings are on the order of the particle diameter at w_m, i.e., $b(w_m) \sim d$.

Figure 10 shows the column width w_m for which the potential energy is minimized at fixed L, as a function of L. Small squares correspond to the results for a two-dimensional hexagonal lattice, the large squares to a four layer thick hexagonal lattice, the crosses to a bct lattice with a four layers thickness (small crosses), eight layer thickness (medium crosses), and sixteen layer thickness (large crosses). Each point is obtained by finding the minimum in the energy versus column width at fixed L in analogy to the inset of Fig. 4. Figure 10 shows a linear relationship between w_m and L in all cases.

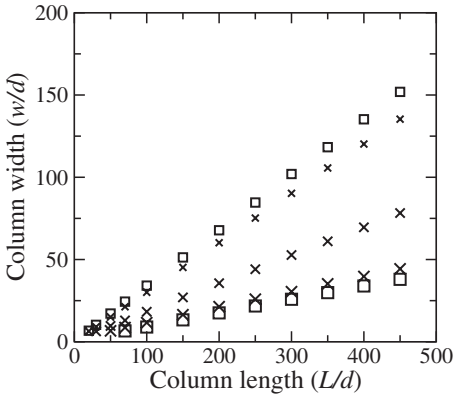

FIG. 10. The minimum energy column width as functions of the column length. The small squares are for the 2D hexagonal lattice and the large squares for four-layer thick hexagonal lattice. The crosses are for the bct lattices with thickness 4 (small circles), 8 (medium), and 16 (large).

To summarize, a linear relationship between w_m and L is established both in experiments (Fig. 9) and through constrained energy minimization by assuming that all columns are identical. However, the calculated ratio w_m/L does not agree with the experiments.

Furthermore, they even show qualitatively different behaviors. It is shown earlier in experiments that the selected column widths are insensitive to the sample thicknesses. This is concluded from not only the using of tubes with different thickness but also the manipulation of initial thicknesses of the aggregations in a sample tube. On the other hand the calculations show clearly that, in different slopes in Fig. 10, the minimizations of the dipole-dipole interactions select different column widths for different sample thicknesses.

We have not be able to exactly pinpoint the reason why minimization of the dipole-dipole interaction predicts columnar widths w that are different from those seen in the experiments. It is possible that the dynamically selected column widths depend to a certain extent on the details of the initial breakup of the aggregate. If this is the case, short-range interactions such as van der Waals attraction or steric repulsion could be important in the early stages of break up and alter the asymptotically selected width. The details of the break up process, however, are unlikely to contribute to the inter columnar spacing which, once the columns are separated, should solely depend on the long range dipole-dipole interaction. A second possible source for the discrepancy is particle packing within the initial aggregate. It is very likely that the break up process is initiated by a complicated interplay between particle packing configuration (possibly including randomness), dipole-dipole interactions, and short-range forces. We leave the study of the early stages of break up to future research.

V. CONCLUSION

We have demonstrated experimentally and numerically a linear relationship between both column width and inter column spacing to chain length in an ensemble of uniaxial dipoles in a quasi-two-dimensional configuration. The observed column spacing b is approximately equal to the chain length L. This spacing is seen to correlate with the crossover distance in the calculated potential energy between two identical columns from slow decay at short distances to fast $1/r^3$ decay of the dipolar repulsion at long distances. We argue that the quick drop of dipolar force sets the scale for the observed stationary intercolumn spacing.

Columnar widths that minimize dipole-dipole interactions w_m are also calculated, and shown to be proportional to the column length L. However the ratio between w_m and L depends strongly on the column thickness and the specific particle packing within the column. This is in disagreement with the experiments which consistently show that $w_m \approx 0.3L$ in a range of different conditions. We offer as possible explanation that the details of the early stages of breakup of the aggregate determine the dynamically selected column width. If this is the case, various short range interactions among particles not included in the energy minimization should play important roles in determining w.

ACKNOWLEDGMENTS

Support by the National Science Council of Taiwan and NSERC Canada is acknowledged.

[1] P. N. Pusey and W. van Megen, Nature (London) **320**, 340 (1986); D. Rosenbaum, P. C. Zamora, and C. F. Zukoski, Phys. Rev. Lett. **76**, 150 (1996).
[2] R. E. Rosensweig, *Ferrohydrodynamics*, 1st ed. (Dover, New York, 1997).
[3] T. C. Halsey and W. Toor, Phys. Rev. Lett. **65**, 2820 (1990).
[4] T. J. Chen, R. N. Zitter, and R. Tao, Phys. Rev. Lett. **68**, 2555 (1992).
[5] T. C. Halsey and W. Toor, J. Stat. Phys. **61**, 1257 (1990).
[6] R. Tao and J. M. Sun, Phys. Rev. Lett. **67**, 398 (1991).
[7] E. Lemaire, Y. Grasselli, and G. Bossis, J. Phys. II **2**, 359 (1992); Y. Grasselli, G. Bossis, and E. Lemaire, *ibid.* **4**, 253 (1994).
[8] J. Liu, E.M. Lawrence, A. Wu, M. L. Ivey, G. A. Flores, K. Javier, J. Bibette, and J. Richard, Phys. Rev. Lett. **74**, 2828 (1995).
[9] H. Wang, Y. Zhu, C. Boyd, W. Luo, A. Cebers, and R. E. Rosensweig, Phys. Rev. Lett. **72**, 1929 (1994).
[10] L. Zhou, W. Wen, and P. Sheng, Phys. Rev. Lett. **81**, 1509 (1998).
[11] M. Fermigier and A. P. Gast, J. Colloid Interface Sci. **154**, 522 (1992).
[12] D. Wirtz and M. Fermigier, Phys. Rev. Lett. **72**, 2294 (1994).
[13] S.Y. Yang,, Y. H. Chao, and H. E. Horng, J. Appl. Phys. **97**, 093907 (2005).
[14] A. Satoh, R. W. Chantrell, S.-I. Kamiyama, and G. N. Coverdale, J. Colloid Interface Sci. **178**, 620 (1996).
[15] M. Gross and S. Kiskamp, Phys. Rev. Lett. **79**, 2566 (1997).
[16] C.-J. Chin, S. Yiacoumi, and C. Tsouris, Langmuir **17**, 6065 (2001).